REMARKS

At the outset, applicants thank the Examiner for her time and consideration of the present application at the interview with the undersigned and in subsequent discussions.

Claims 1, 8-9, 11, 21-26 are pending in the present application. Claim 1 has been amended to further characterize the inhibitor, anti-inhibitor and type of cells utilized in the claimed method. The new recitations in claim 1 were previously recited in claims 4 (in part) and 18. Support for new claims 21-26 may be found in claims 2-7, 10 and 12-20. In addition, support for the new claims may be found at page 5, lines 25-30 and page 10, lines 1-10. As to the recitation to antivin in new claim 21, antivin is a member of the TGF-β family. For the Examiner's convenience, an article by Thisse et al confirming that antivin is a member of the TGF-β family is attached herewith. Thus, it is believed that this recitation is supported throughout the specification (e.g., see pg. 9, lines 30-33). Claims 2-7, 10 and 12-20 have been canceled.

Claims 1-16 and 18-20 were rejected under 35 USC §112, first paragraph, for allegedly failing to comply with the written description and enablement requirements. These rejections are respectfully traversed.

Applicants believe that the claimed invention is fully supported by the present disclosure. Independent claim 1 recites administering to human stem cells an effective amount of an

inhibitor of cell proliferation of cell development in sequential combination with an anti-inhibitor in a controlled manner to maintain the non-differentiated state of stem cells, while allowing their cell division, wherein the anti-inhibitor is anti-TGFβ in an amount of 0.1 µg to 10 mg/ml (present specification, pg. 7, lines 9-15), and wherein said inhibitor is TGFβ in an amount of 0.01 pg/ml to 1 mg/ml (present specification, pg. 9, lines 30-33)and said human stem cells are CD34+ stem cells (see example and figures). In particular, the Examiner's attention is directed to Figure 1A and 1B, which show that under culture conditions according to the claimed invention, a higher percentage of CD34+ cells are observed as compared to culture conditions without TGF-β.

Claim 21 recites administering to human stem cells an effective amount of an inhibitor of cell proliferation of cell development in sequential combination with an anti-inhibitor in a controlled manner to maintain the non-differentiated state of stem cells, while allowing their cell division, wherein the anti-inhibitor is anti-TGFβ in an amount of 0.1 µg to 10 mg/ml (present specification, pg. 7, lines 9-15), and wherein said inhibitor is TGFβ in an amount of 0.01 pg/ml to 1 mg/ml (present specification, pg. 9, lines 30-33) and said human stem cells are haematopoietic stem cells or embryonic stem cells (present specification, pg. 2, lines 30-35).

Thus, claims 1 and 21 recite homogenous populations of cells, inhibitors, and anti-inhibitors that are taught and/or exemplified in the present specification. As a result, applicants believe that the claimed invention is fully supported by the present disclosure.

Claims 1-16 and 19 were rejected under 35 USC §102(b) as allegedly being anticipated by XI et al. These rejections are respectfully traversed. Claims 1, 2, 4, 5-9, 12 and 14 were rejected under 35 USC §102(e) as being anticipated by MOORE et al. Claims 1-10 and 12 were rejected under 35 USC §103(a) as allegedly being unpatentable over HATZFELD et al.

Applicants believe that the present amendment overcomes these rejections. As noted above, independent claim 1 has been amended to incorporate the recitations of claims 4 (in part) and 18. As claim 18 was not rejected on the basis of these publications and was free of prior art, applicants believe that the present amendment obviates the rejections.

In view of the present amendment and the foregoing remarks, therefore, applicants believe that the present application is in condition for allowance, with claims 1, 8, 9, 11 and 21-26 as presented. Allowance and passage to issue on that basis is respectfully requested.

The Commissioner is hereby authorized in this, concurrent, and future replies, to charge payment or credit any overpayment to Deposit Account No. 25-0120 for any additional fees required under 37 C.F.R. § 1.16 or under 37 C.F.R. § 1.17.

Respectfully submitted,

YOUNG & THOMPSON

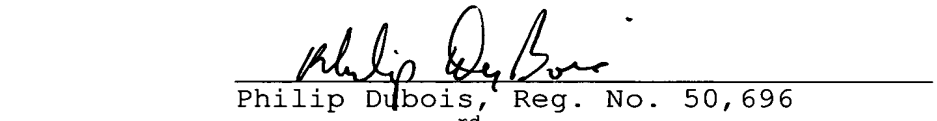

Philip Dubois, Reg. No. 50,696
745 South 23rd Street
Arlington, VA 22202
Telephone (703) 521-2297
Telefax (703) 685-0573
(703) 979-4709

PD/lrs

APPENDIX:

The Appendix contains the following item:

- article by Thisse et al. entitled "Antivin, a novel and divergent member of the TGFβ superfamily, negatively regulates mesoderm induction"

Development 126, 229-240 (1999)
Printed in Great Britain © The Company of Biologists Limited 1998
DEV2332

Antivin, a novel and divergent member of the TGFβ superfamily, negatively regulates mesoderm induction

Christine Thisse and Bernard Thisse

Institut de Génétique et de Biologie Moléculaire et Cellulaire, CNRS/INSERM/ULP, BP 163, 67404 Illkirch Cedex, CU de Strasbourg, France
Address for correspondence (e-mail: thisse@igbmc.u-strasbg.fr)

Accepted 27 October; published on WWW 14 December 1998

SUMMARY

Mesoderm induction and patterning are mediated by members of the TGFβ superfamily. We have isolated a novel zebrafish member, *antivin*, that structurally is highly related to mouse *lefty*. Overexpression of *antivin* completely abolishes mesoderm induction at blastula stage, yet resultant embryos develop well-patterned epidermal and neural derivatives. The mesoderm-inhibiting activity of *antivin* can be mimicked by *lefty* and is suppressed by increasing levels of the mesodermal inducer Activin or its receptors. On the basis of its expression and activity, we propose that Antivin normally functions as a competitive inhibitor of Activin to limit mesoderm induction in the early embryo.

Key words: Antivin, Mesoderm, Induction, TGFβ, Activin, Zebrafish

INTRODUCTION

Understanding the molecular basis of cellular interactions that generate the animal body plan represents a major goal in developmental biology. Inductive interactions in which one cell group influences the fate of neighboring cells, constitute one of the major strategies used to produce diverse cell types during vertebrate embryogenesis.

In the past years, much attention has been focused on the formation of the mesoderm which, in *Xenopus*, derives from the marginal zone and depends upon inductive signals emanating from the endoderm. A number of molecules have been implicated in providing the mesoderm-inducing signal(s) or in setting up a range of dorsoventral mesodermal cell fates. These include members of the Wnt family (reviewed in Kimelman et al., 1992), FGFs (Kimelman and Kirschner, 1987) and molecules belonging to the TGFβ family such as Activin and Vg1. Activin itself, when overexpressed, induces a wide variety of mesoderm derivatives in a dose-dependent manner. Low doses of Activin induce the expression of ventroposterior mesodermal markers, whereas high doses lead to the induction of dorsoanterior specific markers (Thomsen et al., 1990; Green et al., 1992). Moreover, recent studies suggest that Activin can function as a diffusible morphogen to elicit differential gene expression and cell fate depending on its concentration (Green et al., 1992; Gurdon et al., 1994).

Although current work is directed towards identifying new molecules involved in mesoderm induction and describing their developmental effects, little is known about the regulation of mesodermal induction and establishment of the Activin morphogen gradient. Insight into the mechanisms that regulate the activity of other TGFβ-related-molecules acting as morphogens was provided by studying the control of dorsoventral patterning by BMPs. It was shown that the morphogenetic activity of BMPs is limited by their interaction with three proteins secreted by the organizer, Chordin, Noggin and Follistatin, which bind to BMP2/4, preventing them from interacting and stimulating their receptors (for review Thomsen, 1997).

Here, we present evidence that the morphogenetic activity of Activin, another member of the TGFβ superfamily, can also be modulated. We describe the isolation in zebrafish, of a novel signaling molecule, called Antivin (Atv) which belongs to a new subgroup of the TGFβ superfamily. Overexpression of Atv leads to a dramatic depletion of mesendoderm subpopulations in a dose-dependent manner. This inhibitory effect of Atv can be suppressed by increasing doses of the mesodermal inducing factor, Activin or its receptors. These results strongly suggest that Atv functions as a competitor of the Activin signaling pathway to limit mesoderm induction at blastula stage in the zebrafish embryo.

MATERIALS AND METHODS

Whole-mount in situ hybridization

Whole-mount in situ hybridizations were performed according to Thisse et al. (1993). The antivin antisense RNA probe was generated from the full-length cDNA subcloned in pBSIISK+, using the T7 RNA polymerase after *Not*I digestion. A second probe, which corresponded to a 287 pb 3′ non-coding fragment generated by a *Ssp*I digestion gave the same pattern of expression.

Most of the probes used in this study were isolated from a large-

scale in situ hybridization screen (unpublished data). The mesodermal probes were BR146, a marker specific of paraxial mesoderm at gastrulation, and *draculin*, which is specifically expressed in the hematopoetic lineage from blastula stage to late embryogenesis.

The endodermal probes were *axial* (Strähle et al., 1993), which is expressed in axial mesoderm and in endodermal cells at gastrulation and DS507, a cDNA encoding the transcription factor *Gata5*, which is specifically expressed into presumptive endodermal cells at blastula and gastrula stages.

The ectodermal probes corresponded to AS11, a cDNA specifically expressed in the presumptive brain and the marginal territory at blastula and gastrulation stages, and BR138, a cDNA that encodes the carboxy-terminal part of the zebrafish homolog of the mammalian vHNF1 transcription factor, specific of the posterior hindbrain and dorsal spinal cord from mid-gastrulation to early somitogenesis. Finally, the DS363 cDNA codes for the zebrafish *neurogenin1* homolog. This gene is expressed in proneural clusters of the hindbrain, spinal cord and trigeminal ganglia after mid-gastrulation.

All probes were synthesized using the T7 RNA polymerase, after linearizing the template DNA with *Not*I.

RNA injections

Atv, lefty, activin receptor type IIa and TARAM A^D cDNAs were inserted into the expression vector pCS2+ and linearized with *Not*I. Activin βB cDNA inserted in pSP64T was linearized using *Xba*I. Capped synthetic RNAs were in vitro transcribed using the Stratagene in vitro transcription kit. Injections were performed as described in Wittbrodt and Rosa (1994).

Antivin RNA (0.5-250 pg), lefty RNA (1-25 pg), activin βB RNA (20-300 fg), ARIIa RNA (25-500 pg) and TARAM A^D RNA (100-500 pg) were pressure injected in one blastomere of embryos at the 2-cell stage. Injection experiments were performed three times using different RNA synthesis reactions. For each in situ hybridization probe, and at every RNA concentration, more than 100 injected embryos were analyzed. Uninjected siblings and control embryos injected with *E. coli lacZ* RNA (500 pg) were analyzed under the same conditions and did not display any abnormalities.

RESULTS

Zebrafish Antivin is a novel TGFβ family member

To identify genes involved in early patterning of the zebrafish embryo, we have performed a large scale in situ hybridization screen of random cDNA clones for spatially restricted patterns of expression. One early expressed gene, *antivin* (*atv*), shared sequence similarities with members of the TGFβ superfamily. Analysis of the predicted amino-acid sequence of corresponding full-length cDNA clones (Fig. 1A,B) revealed that Atv was more closely related to TGFβ1 and TGFβ2 than to BMPs. However, significant differences in protein sequence and predicted structure indicate that Atv belongs to a new subclass in the TGFβ superfamily (Fig. 1B) that also contains mouse Lefty (Meno et al., 1996; Oulad-Abdelghani et al., 1998) and the human Endometrial bleeding associated factor, Ebaf (Kothapalli et al., 1997). The sequence landmarks of the TGFβ superfamily such as the six cysteines grouped into a 'cysteine knot' (Daopin et al., 1992; Schlunegger and Grutter, 1992) or the four strands of anti-parallel β sheets which emanate from the knot and form two fingers-like projections (Fig. 1C) are present in Atv, Lefty and Ebaf. However, these three proteins lack the large α helix required for dimerization with other TGFβ members as well as the cysteine involved in the covalent stabilization of these homodimers or heterodimers

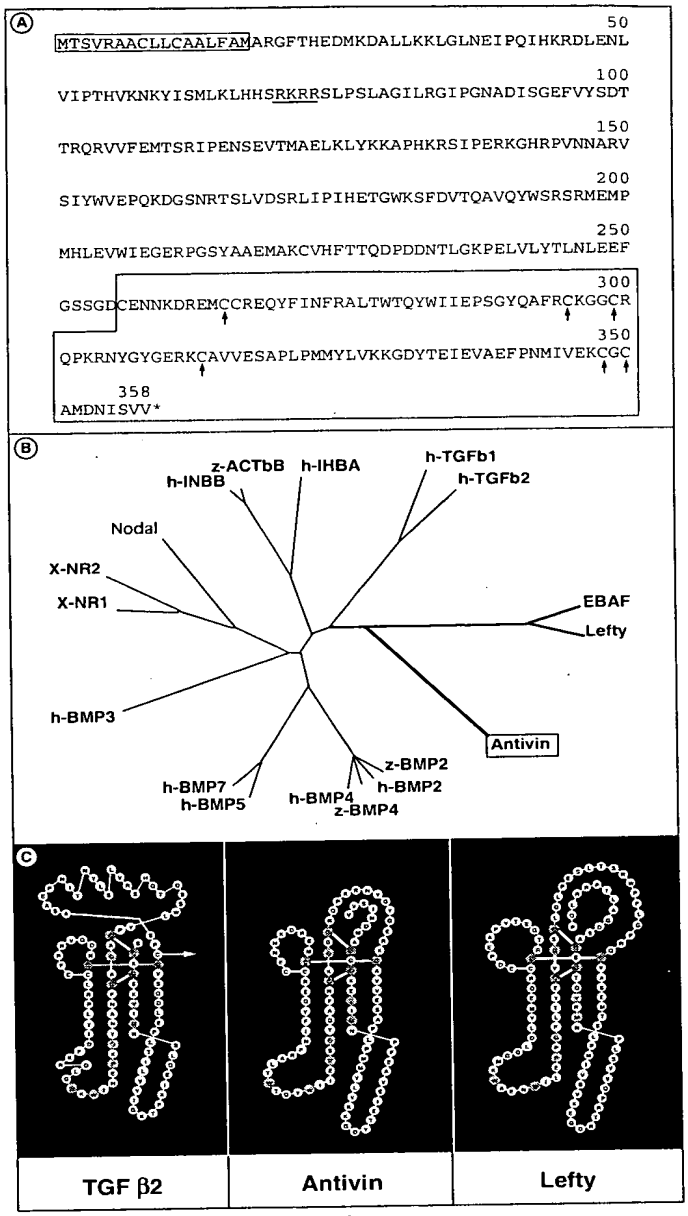

Fig. 1. Amino-acids sequence of Antivin and structural relationships with other members of the TGFβ superfamily. (A) Primary sequence of Atv. Amino-acid numbering on the right. Signal peptide boxed, putative cleavage site underlined with bold line. Conserved cysteine residues indicated with arrows and carboxy-terminal domain containing the cysteine residues boxed with bold line.
(B) Philogenetic tree illustrating the relationship of Atv with other members of the TGFβ superfamily. The amino-acid sequences of the conserved carboxy-terminal domain shown in B were compared using the ClustalW alignment program. The various sequences are from the GenBank and Swissprot databases. This analysis shows that Atv defines, with Lefty and Ebaf, a new subclass within the TGFβ superfamily. (C) Comparison of the secondary structure predicted by computer analysis of the carboxy-terminal domain of Atv and Lefty with the known secondary structure of the TGFβ2. Amino-acids identical in all TGFβ superfamily members in red, amino-acids presenting conservative substitutions in pink. The dimerization bound is schematically shown by a green arrow.

(Fig. 1C). In place of the missing α helix, they display a long carboxy-terminal tail emanating from the cysteine knot.

TGFβ-related members are synthesized as pro-proteins and subsequently cleaved at a dibasic RXXR site (Barr, 1991). The only putative cleavage site in the Atv sequence is a RKRR motif located at a position amino-acids 71-74 (Fig. 1A), comparable to the proteolytic cleavage sites of Lefty and Ebaf (amino-acids 74-77). These cleavage sites are located close to amino-terminus and, as a consequence, the mature peptides of these three proteins (286-291 AA) are twice as long than those of other TGFβ family members (110-140 AA).

Sequence analysis reveals that Atv shares only 35.3% amino-acid identity with Lefty and 35.5% with Ebaf, whereas Lefty is 78.3% identical to Ebaf if one compares the whole sequence. This low level of sequence similarity between Atv and Lefty/Ebaf is also observed within the cysteine domain (boxed in Fig. 1A) as Atv displays only 35.1% of amino-acid identity with Lefty, or 39.4% with Ebaf, but 42.9% with h-TGFβ1. In contrast, Lefty and Ebaf are 82.7% identical in their cystein domains. These observations suggest that *atv* does not represent the zebrafish *lefty* or *ebaf* orthologous gene and is a novel TGFβ family member.

Dynamic expression of *antivin* during embryonic development

Expression of *atv* is first detected after the midblastula transition in cells at the dorsal blastoderm margin which later gives rise to the zebrafish equivalent of the organizer (Fig. 2A). During late blastula stages, expression spreads around the margin (Fig. 2B,C), but then, decreases progressively during gastrulation, except in the dorsalmost region. In the gastrula midline, *atv* is expressed in cells at the leading edge of the mesendoderm, that extends anteriorly under the ectoderm to form the prechordal plate (Fig. 2D). In contrast, more posterior axial mesoderm fails to maintain expression (Fig. 2D,E). In addition, atv transcripts are detected in ectodermal cells overlying the posterior part of the *atv* mesendodermal domain (Fig. 2D). The ectodermal domain of *atv* expression gradually extends within the neurectoderm both anteriorly, following the migration of the prechordal plate towards the animal pole, and dorsally (Fig. 2E).

At the onset of somitogenesis, *atv* continues to be expressed in the ventral forebrain region (Fig. 2F) yet disappears from this region by the 10-somite stage. However, starting at the 7-somite stage, a new expression domain can be detected in the posterior part of the notochord (Fig. 2G). This expression extends anteriorly and reaches the tip of the notochord by the 14-somite stage. At the same time, this expression starts to disappear from the posterior third of the notochord (Fig. 2H) whereas transcripts are found in the most caudal axial mesoderm until the end of the tail elongation.

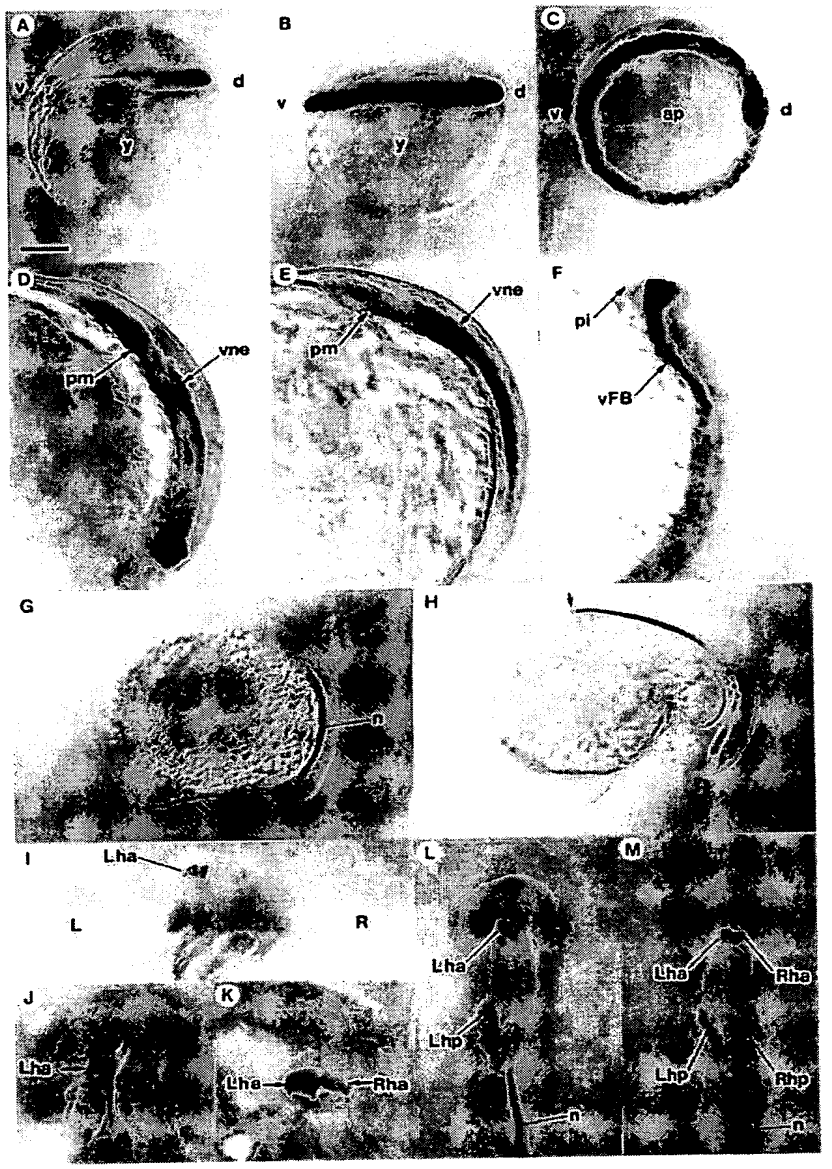

Fig. 2. Distribution of *antivin* transcripts during embryogenesis. (A) *atv* transcripts are first detected at the sphere stage at the dorsal margin of the embryo. (B,C) 40% epiboly. In lateral view in B and polar view in C, *antivin* RNA is localized all around the margin. (D) At gastrulation, *atv* is expressed in the prechordal mesendoderm (pm) and in the overlying ventral neurectoderm (vne). (E) As the mesoderm expressing *atv* migrates anteriorly, labelling increases in the neurectodermal layer. (F) At the onset of somitogenesis, *atv* expression is located in the ventral forebrain (vFB) territory. (G) At the 10-somite stage, *atv* starts to be expressed in the caudal part of the notochord (n). (H) By the 16-somite stage, anterior notochord cells (arrow) express *atv*, while transcripts disappear posteriorly. (I) At the 20-somite stage, optical cross-section of the diencephalon showing *atv* expression in the left habenula nucleus (Lha). (J) In 92.8% embryos, *atv* is expressed in the left part of the habenula. (K) In 4.5% embryos, both left and right sides of the habenula are labelled. (L) When located in the left part of the habenula, *atv* is also expressed in the left heart primordium (Lhp). (M) When located on both sides of the habenula, *atv* is also seen in both left and right heart primordia. ap, animal pole; d, dorsal; L, left; pi, pillow; R, right; Rha, right habenula; Rhp, right heart primordium; v, ventral; y, yolk. Scale bar, 150 μm (A,B,D,E,G,H,J,K), 300μm (C,F,I,L), 75μm (M-Q).

Finally, by the 18-somite stage, two new domains start to transiently express *atv*, the first being the heart primordium and the second, the diencephalic habenula nucleus (Fig. 2I). At this stage, long before any morphologically visible left-right (L/R) asymmetry, 92.8% (443/477) embryos display restricted *atv* expression in the left part of the habenula (Fig. 2I,J), as well as in the left heart primordium (Fig. 2L). However, in 1.9% (9/477) embryos, labelling is detected in the right part of the habenula and right heart primordium and in 4.5% (25/477) embryos, expression is seen in both left and right parts of the habenula and heart primordia (Fig. 2K,M). By the 25-somite stage, atv transcripts disappear from the heart primordium while expression in the habenula ceases by 24 hours of development.

In summary, *atv* expression domains correlate with regions known to be crucial for inductive processes. It is expressed at the blastula margin in place and at time of mesoderm induction, in the axial mesendoderm where vertical induction takes place and in tissues known to send out inductive signals such as notochord and heart primordium. As Atv belongs to a family of signaling molecules, its expression pattern suggests that this factor may be involved in these inductive signaling pathways or their regulation.

Dose-dependent loss of mesendodermal derivatives following *antivin* overexpression

To investigate Atv function, in vitro synthesized RNA (1-25 pg) was injected into 2-cell-stage embryos. The range of observed defects correlated with the amount of injected RNA. These alterations were first identifiable morphologically at gastrulation. Embryos injected with low levels of RNA (1 pg) were characterized by a shortening of the embryonic axis and an associated anterior thickening (Fig. 3D). At early somite stages, the thickening was located in the prospective head region (Fig. 3E). Later, these embryos displayed a depletion of cephalic mesoderm associated with a

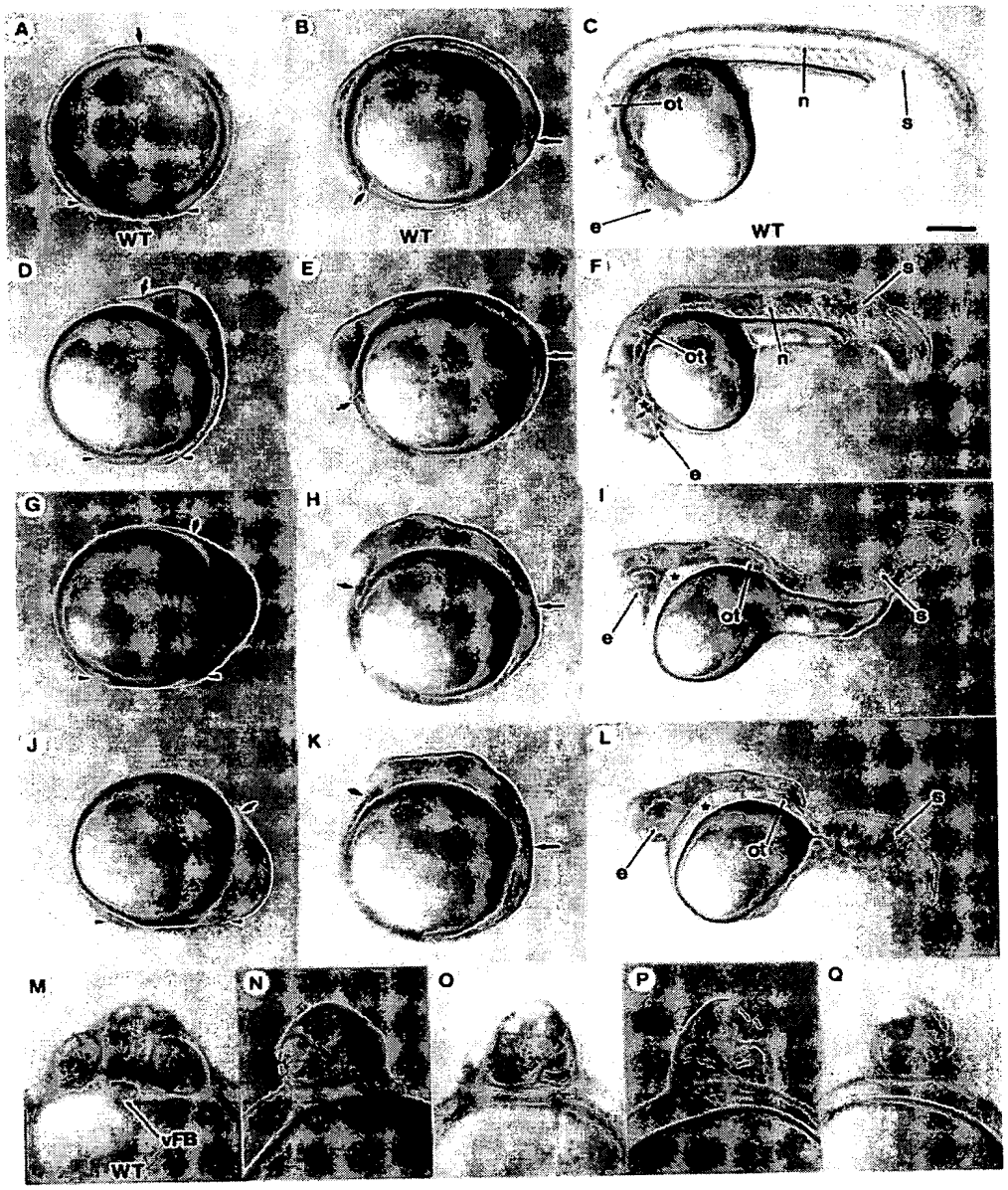

Fig. 3. Morphological defects induced by Antivin overexpression. (A-C,M) Wild-type control (WT). (D-F) Weak phenotypes; (G-I) intermediate phenotypes; (J-L) strong phenotypes; (N-Q) range of head defects. (A,D,G,J) Gastrulation stage; (B,E,H,K) somitogenesis; (C,F,I,L) 36 hours of development. (D) Embryos injected with a low dose of antivin RNA (1 pg) are characterized by a shortening and anterior thickening of the embryonic axis. (E) This thickening is located in the prospective head during somitogenesis. (F) The resulting embryos display a lack of cephalic mesoderm (star) and a range of cyclopia phenotypes as detailed in N-Q. (G,H) For intermediate doses of RNA (2 pg), the embryos display a thicker and shorter embryonic axis. (I) The derived embryos lack the ventral part of the forebrain, have an unique cyclopic eye (e) and the head is devoid of all mesodermal structures (star). In the absence of notochord, somites (s) fuse under the neural tube. (J) For embryos injected with higher doses of RNA (5 pg), cells accumulate at the margin. (K) The yolk plug closure is located behind the cephalic region. (L) Embryos are defective in all ventral part of the CNS and all mesodermal derivatives of the head and trunk (star). (M-Q) Details of the deletion in the forebrain. The optical vesicles appear closer (N), fused (O-P) or a unique vesicle is formed (Q). Small arrows show the anterior tip of the embryonic axis. Long arrows, position of the yolk plug closure; arrowheads, position of the gastrula margin; n, notochord; ot, otic vesicule. Scale bar: 150 μm (A-C,G,H,L,M); 75 μm (D-F,I-K).

range of eye defects and cyclopia resulting from the deletion of the ventral forebrain (Fig. 3F,N-Q).

Embryos injected with intermediate levels of RNA (2 pg) displayed an even thicker and shorter axis (Fig. 3G-H), severe cyclopia and a head completely devoid of mesodermal structures (Fig. 3I). In addition, the notochord was absent in the trunk and tail, resulting in the medial fusion of somites (Fig. 3I).

Embryos injected with higher RNA levels (5 pg) had an accumulation of cells close to the margin (Fig. 3J) and the site of the yolk plug closure was located behind the cephalic region (compare Fig. 3K with B). Histological sections revealed that these embryos were totally devoid of hypoblastic cells. Later, these embryos lacked all structures normally derived from endoderm and mesoderm in their head and trunk (Fig. 3L). In the tail, a few somites were variably formed. Finally, injection of 25 or more pg of RNA resulted in embryos that differentiated only epidermis, dorsal brain and displayed an atrophic, undifferentiated tail (not shown).

Ectodermal differentiation in the complete absence of mesendoderm

To correlate defective gastrulation with late phenotypes, embryos were first analyzed by in situ hybridization for the expression of mesendodermal markers at gastrulation. Endoderm was revealed to be the most sensitive to Atv overexpression. As shown with *axial* and *gata5* (Fig. 4A-D), this tissue was strongly reduced at very low doses (0.5 pg, Fig. 4C,D) and absent for higher amount of antivin RNA (1 pg, Fig. 4A,B). As well, the anterior prechordal plate was always deleted as assayed using *hgg1* (Fig. 4E,F) which encodes the zebrafish Cathepsin L (Thisse et al., 1994). Intermediate (2 pg) or high doses of RNA (5-25 pg) caused additional depletions of mesendodermal subpopulations. 2 pg antivin RNA led to the absence of axial mesoderm. This was shown by examining expression of *no tail* (Schulte-Merker et al., 1992) which is specific to the marginal region and presumptive notochordal territory (Fig. 4G,H). Injection of 2 pg antivin RNA also resulted in the absence of paraxial mesoderm as shown with *BR146*, which encodes a proteoglycan specific to this territory at gastrulation (Fig. 4I,J). For higher doses of RNA (5-25 pg), depletion of ventral mesoderm also occurred. Ventral mesoderm appeared reduced in size (5 pg, Fig. 4K,L) or completely absent (25 pg) as shown by *draculin*, which

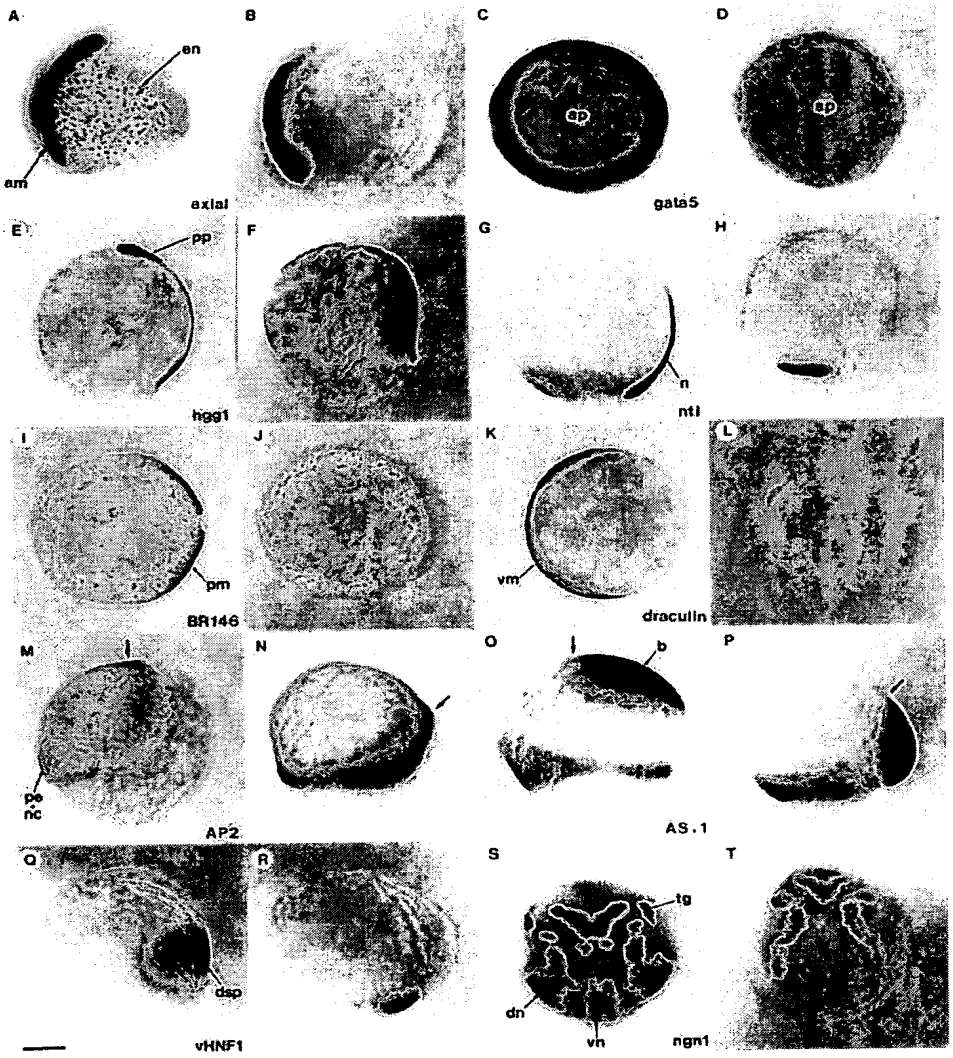

Fig. 4. Antivin inhibits mesoderm formation at gastrulation. Embryos injected with antivin RNA were analyzed by in situ hybridization with different molecular probes. For each probe, the wild-type sibling and the corresponding injected embryo are shown next to each other (left and right, respectively). (A,B) Labelling with *axial* and (C,D) labelling with *gata5* for low doses of antivin RNA (1 pg or 0.5 pg, respectively) showing the deletion (A,B) or strong reduction (C,D) of endoderm (en) during gastrulation. (E,F) Labelling with *hgg1*, a marker of anterior prechordal plate (pp) and yolk syncytial layer. (F) Overstaining with *hgg1* reveals the absence of prechordal plate in *atv*-injected embryos. (G,H) Absence of axial mesoderm is revealed using *ntl*, which labels the notochord (n) as well as the margin. (I,J) Absence of paraxial mesoderm (pm) is detected probing with *BR146*. (K,L) *draculin*, a marker of ventral mesoderm (vm) reveals that *atv*-injected embryos lack this territory. (M,N) Expression of *AP2*, specific to presumptive epidermis (pe) and neural crest (nc), is enlarged and shifted dorsovegetally (arrow). (O,P) The presumptive brain (b), labelled with *AS11*, is located at the margin rather than at the animal pole. (Q,R) Expression of *vHNF1*, which marks the presumptive dorsal spinal cord (dsp), is shifted to the lateral margin. (S,T) Expression of *neurogenin1* (ngn1) reveals the presence of proneural clusters except in the ventral midline. Arrows show the anterior tip of the embryonic axis. dn, dorsal proneural clusters; tg, trigeminal ganglion; vn, ventral proneural clusters. Scale bar: 150 μm.

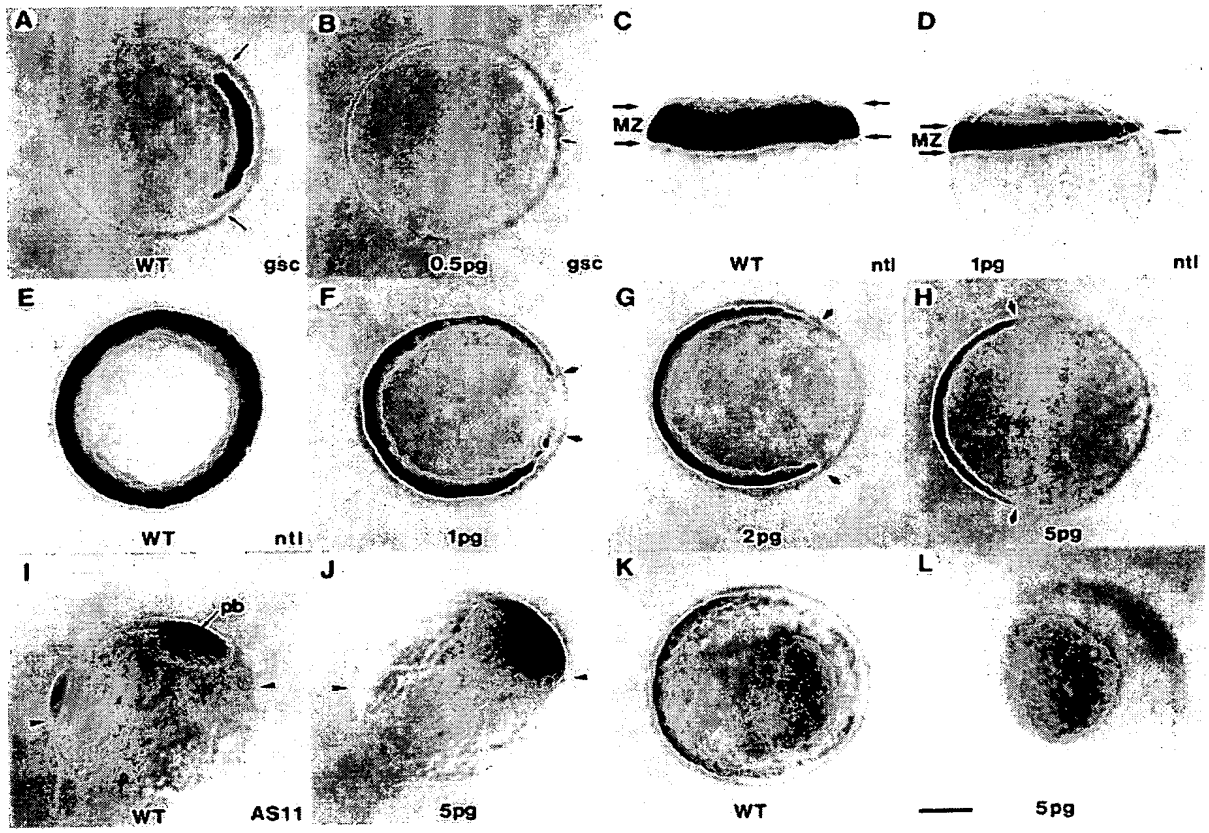

Fig. 5. Antivin inhibits mesoderm induction at blastula stage. Wild-type control embryos (A,C,E,I,K) and embryos injected with 0.5 pg (B), 1 pg (D,F), 2 pg (G), 5 pg (H,J,L) antivin RNA were analyzed by in situ hybridization with a marker of prechordal mesoderm, *gsc* (A,B), a panmesodermal marker, *ntl* (C-H) or the *AS11* marker which labels the margin and the presumptive brain territory (I-L). (B) Injection of antivin RNA inhibits *gsc* expression (delimited by arrows). (D) Lateral view of an embryo depicting the loss of *ntl* expression in the marginal zone (MZ, delimited by arrows) along the animal to vegetal pole axis. (F-H) Increasing doses of antivin RNA lead to a progressive deletion (arrows) of the presumptive mesoderm. (H) Detectable expression of *ntl* is located in cells fated to form the tail bud. (J-L) Labelling with AS11 confirms the complete loss of the marginal zone. Expression of AS11 in presumptive brain (pb) extends down to the margin (arrowheads). Embryos are shown in polar views, except for C,D,I,J, which are lateral views. Scale bar: 150 μm.

encodes a poly-zinc finger protein specific to the hematopoetic lineage, a population of cells deriving from the ventral-most mesoderm. In summary, Atv overexpression leads to a dose-dependent depletion of mesendoderm at gastrulation.

Despite the absence of mesendoderm, ectodermal structures differentiated, although were displaced. For example, expression of zebrafish *AP2* (Fürthauer et al., 1997) in presumptive epidermis and neural crest (Fig. 4M) was expanded. The anterior-most extent of expression was located at the tip of the hypertrophic embryonic axis and was shifted dorsovegetally (Fig. 4N). The animal pole expression of *AS11*, an early marker of the presumptive brain (Fig. 4O), was located near the margin rather than anteriorly (Fig. 4P). Histological sections of these embryos revealed that the hypertrophic embryonic axis contained only cephalic neurectodermal cells (data not shown). The truncal neurectoderm was also examined using the zebrafish homolog of *vHNF1*, which labels the presumptive dorsal spinal cord. In Atv-injected embryos, *vHNF1* expression was shifted to the lateral margin (Fig. 4Q-R). Finally, expression of *neurogenin1* revealed that proneural clusters were formed (Fig. 4S) except those in the ventral midline from which the ventral motor neurons originate (Fig. 4T). Later in development, staining with markers specific to primary neurons, such as *islet1* (Inoue et al., 1994) or *AS28* (Fürthauer et al., 1997) showed dorsal sensory neurons were present while ventral motor neurons were absent (not shown).

In conclusion, in the absence of mesendoderm, cells of embryos overexpressing Atv display an ectodermal fate at gastrulation. The hypertrophic axis from its anterior tip to the dorsal margin has a cephalic neurectodermal identity while the lateral marginal region has acquired a dorsal spinal cord fate in which proneural clusters are properly induced.

Antivin modulates mesodermal induction

To determine if Atv-mediated inhibition of mesoderm formation at gastrulation results from an alteration in the determination of the presumptive mesodermal territory, we analyzed the expression of mesodermal or ectodermal markers at the blastula stage. We first probed the mesodermal layer with *goosecoid* (*gsc*), which marks the dorsal margin (Stachel et al., 1993; Schulte-Merker et al., 1994; Thisse at al., 1994) and later forms the central part of the fish organizer (Fig. 5A,B).

Expression of this marker was dramatically reduced at very low dose of antivin RNA (0.5 pg) and abolished at higher doses (1-25 pg). Similarly, expression of *no tail* was progressively deleted from dorsal to ventral, in a dose-dependent manner (Fig. 5C-H) and appeared progressively thinner along the animal-vegetal axis (Fig. 5C,D). The same observation was made using the mesodermal marker *snail1* (Thisse et al., 1993; Hammerschmidt et al., 1993), which completely disappeared from the margin in a dose-dependent manner. For *evel* (Barro et al., 1995), ventral mesodermal expression disappeared while its expression in presumptive tail bud was still present (not shown).

Further analysis was carried out using *AS11*, which specifically marks the marginal zone and the presumptive brain at the blastula stage. In *atv* overexpressing embryos, while the marginal expression of *AS11* had completely disappeared, the presumptive brain territory extended more vegetally up to the margin (Fig. 5I-L).

These results show that blastula embryos overexpressing *atv* are reduced to structures deriving from the animal zone, a region fated to become ectoderm. The dose-dependent loss of mesoderm and its progressive replacement by presumptive ectodermal territory strongly suggests that Atv modulates mesoderm induction.

Mouse Lefty mimics the Antivin effect

While highly divergent in sequence, modelling of Lefty and Atv reveals a strong similarity in secondary structure, particularly in domains predicted to play an essential role in their spatial conformations. Therefore, we tested the ability of Lefty to substitute functionally for Atv. We found that injection of RNA encoding the mouse *lefty* produces phenotypes indistinguishable from phenotypes obtained after injection of antivin RNA. As for Atv, overexpression of Lefty led to inhibition of mesoderm induction at blastula stage. This strongly suggests that similarities in the spatial conformations of Lefty and Atv are sufficient for the two proteins to carry out essential aspects required for their function.

Activin antagonizes Antivin activity and restores mesoderm induction

While Atv inhibits mesoderm induction, other members of the TGFβ family, such as Activins are known to induce a wide variety of mesoderm derivatives in a dose-dependent fashion (Green et al., 1992). Because of their opposite effect on the mesoderm induction, we hypothetized that Atv negatively interacts with the Activin signaling pathway. If this hypothesis is true, increasing Activin concentration will allow competition of Atv activity and restore mesoderm induction. We first verified that, in zebrafish, Activin βB (Wittbrodt and Rosa, 1994) induces a range of mesoderm derivatives in a dose-dependent manner. Low doses of activin RNA (20 fg) did not affect the prechordal mesoderm (Fig. 6B) but led to an enlargement of posterior axial mesoderm (Fig. 6F). Progressive addition of activin RNA (80-300 fg) resulted in induction of both prechordal and posterior-axial mesoderm (Fig. 6C,D,G,H).

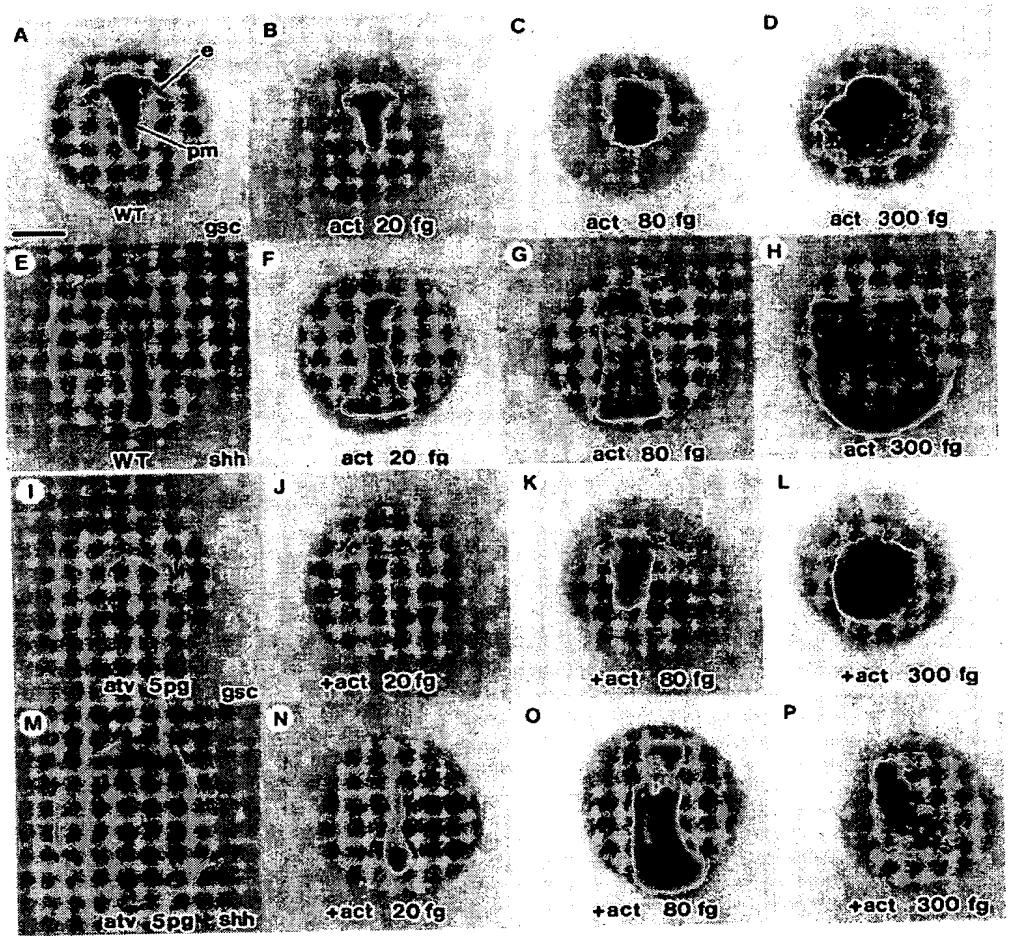

Fig. 6. Activin βB rescues the Antivin-mediated deletion of mesoderm. (A-D) Expression of *gsc*, an anteroaxial mesodermal marker in a wild-type control embryo in A and in embryos injected with increasing doses of activin βB RNA, 20 fg (B), 80 fg (C) or 300 fg (D). (E-H) Expression of *shh*, a marker of posterior-axial mesoderm, in a wild-type control (E) and in embryos (F-H) injected with the same increasing doses of activin βB. (I) Expression of *gsc* at the end of gastrulation in an *atv*-injected embryo. Ectodermal expression of *gsc* is present while prechordal plate mesodermal expression is absent. (J-L) Coinjection of activin βB has no effect at 20 fg while, at higher doses, the prechordal plate expression of *gsc* is rescued or even exaggerately induced. (M) *atv*-injected embryos do not express *shh*. (N-P) Coinjection of increasing doses of activin βB progressively rescues or even strongly induced *shh* expression. e, ectodermal expression of *gsc*; pm, prechordal mesoderm. Scale bar: 200 μm.

To test Activin/Atv interaction, 5 pg of antivin RNA, a dose leading to strong mesoderm depletion (Fig. 6I,M), was injected with increasing doses of activin βB (20-300 fg). Injected embryos were then analyzed by in situ hybridization for the extent of anteroaxial and posteroaxial mesoderm formation. Addition of 20 fg of activin RNA resulted in a partial rescue of chordamesoderm (Fig. 6N) but had no effect on prechordal plate (Fig. 6J). Addition of activin RNA at doses of 80 fg or more, restored and even induced both prechordal and chordamesoderm (Fig. 6K,L,O-P). In a reverse experiment, when 80 fg of activin RNA was injected with increasing doses of antivin RNA (1-25 pg), the strong mesodermal induction mediated by Activin was reduced or even abolished by addition of Atv (not shown). These results further demonstrate that Atv and Activin have antagonistic effects on mesoderm induction, and act in a competitive manner.

The possible activation of *atv* expression by Activin was also investigated. Injection of activin RNA (80 fg–5 ng) rather induces formation of mesendoderm at blastula stage but does not affect *atv* expression (not shown).

These observations show that Atv inhibition of mesoderm induction does not result from a negative feedback loop but strongly suggests that Atv and Activin act at the same level in the cascade of mesodermal induction events.

We also tested whether Atv activates its own expression, by injecting antivin RNA (1-25 pg) and probing these embryos by in situ hybridization with an antivin RNA probe comprising the 3′ UTR. Compared to control embryos, no induction of *atv* can be detected. We conclude that Atv does not activate its own expression.

Activin Receptor type IIa and constitutively activated form of a type I Activin receptor related override Antivin inhibitory effect

To further investigate the interaction between Atv and the Activin signaling pathway, we analyzed the ability for downstream elements to rescue the inhibitory effect of Atv on mesoderm induction. Atv RNA was coinjected at a dose that abolishes mesoderm induction at blastula stage (5 ng) with increasing

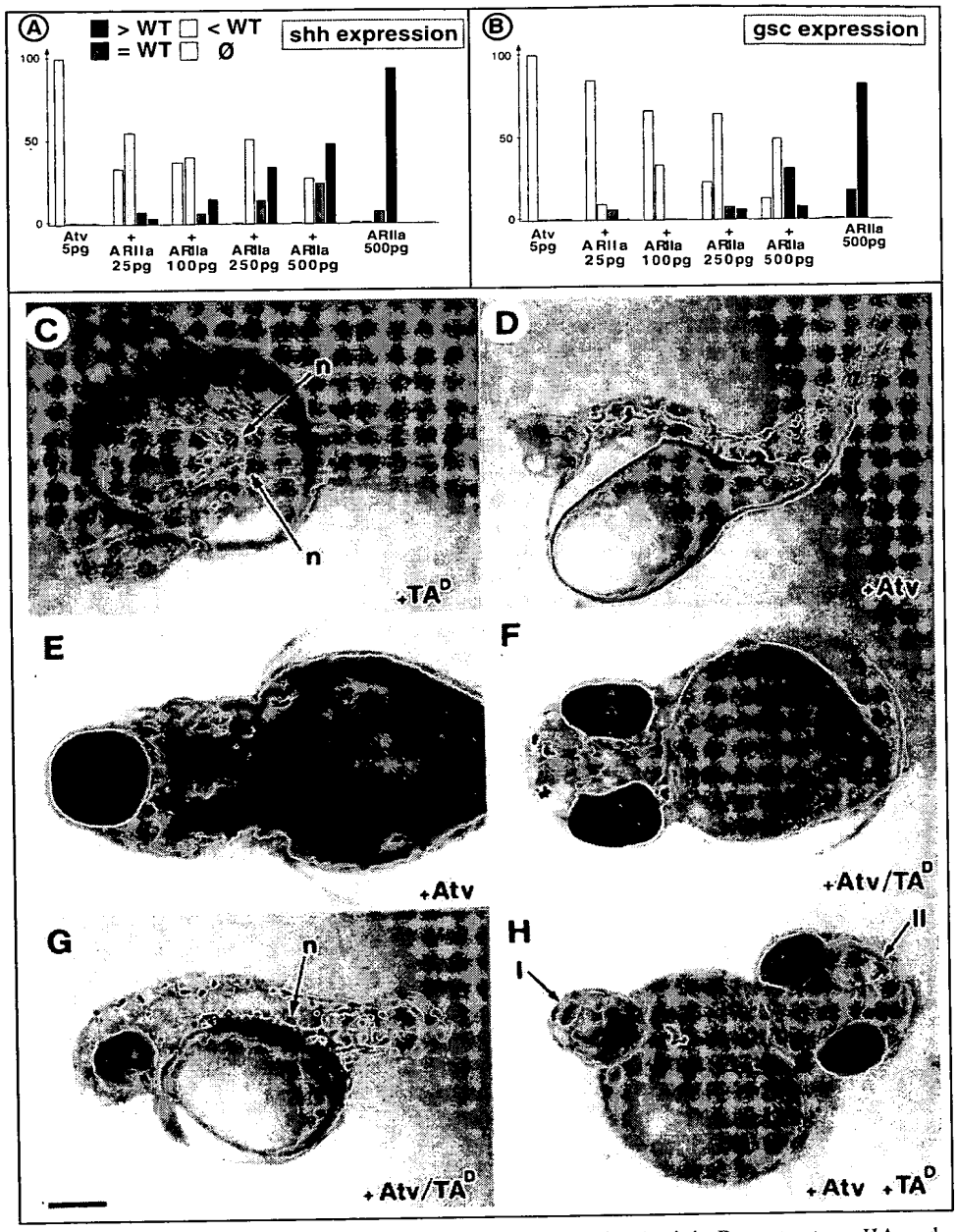

Fig. 7. Rescue of the Antivin-mediated loss of mesoderm by Activin Receptor type IIA and Taram A^D. (A,B) Rescue of the Atv inhibitory effect by coinjection of increasing doses of Activin receptor type IIa. Bars indicate the percentage of embryos displaying an overinduced expression (black), a wild-type expression (red), a reduced expression (yellow), or a complete loss of expression (white) of *shh*, (A), or of *gsc* (B). (C) Embryo injected with 500 pg of TARAM-A^D RNA in one blastomere at the 16-cell stage develops a complete secondary axis including a fully differentiated notochord (n). (D) Embryo injected with 10 pg of antivin RNA showing a lack of all mesendodermal derivatives in head and trunk and an absence of axial mesoderm in tail. (E) Focus on the cyclopia phenotype of an embryo injected with 10 pg of Atv RNA (ventral view). (F) Coinjection of 500 pg of TARAM-A^D RNA rescues Atv-mediated cyclopia phenotype and (G) a differentiated notochord. (H) Front view of an embryo injected with Atv (10 pg) at the 2-cell-stage followed by injection of TARAM-A^D RNA (500 pg) in a marginal blastomere at the 16-cell-stage. Two axes are formed, the primary axis (I) is devoid of mesendoderm and displays a cyclopia phenotype as the result of Atv effect while the secondary axis (II) induced by TARAM-A^D comprises axial mesendoderm and two separated eyes. Scale bar: 150 μm in C,D,G; 100 μm in E,F,H.

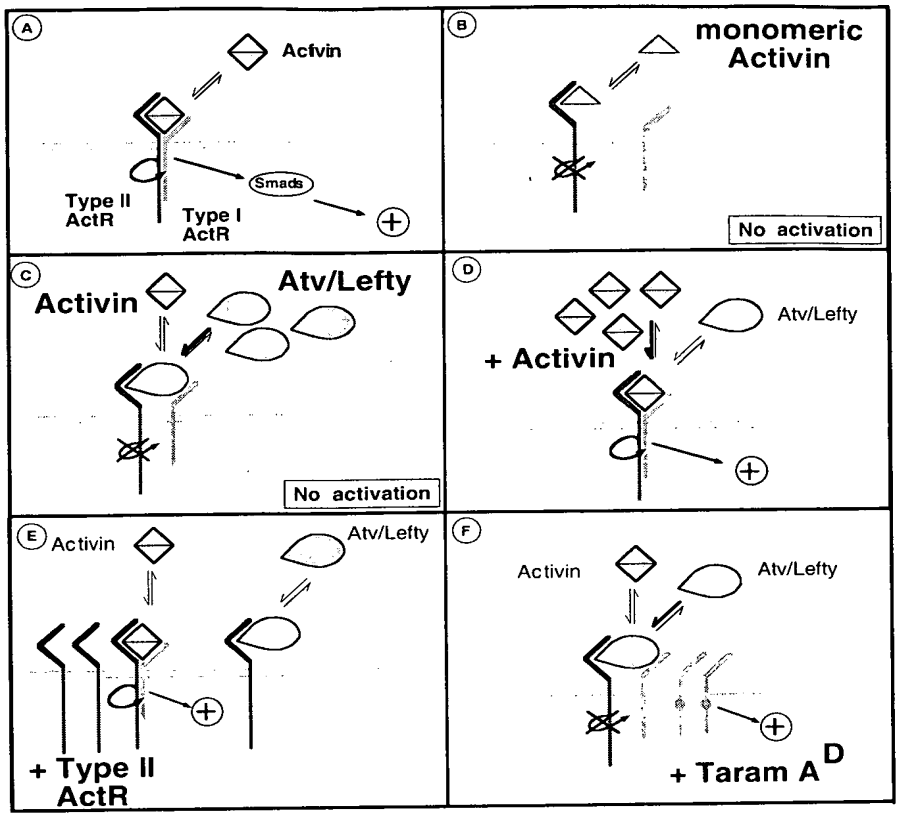

Fig. 8. Model of Antivin/Activin interaction. (A) Schematic representation of TGFβ signal transduction pathway. Ligand, such as dimeric form of Activin, binds to type II receptor, which then recruits a type I receptor. After transphosphorylation of the type I receptor by the kinase activity of the type II receptor, the activated type I receptor transmits the signal to Smad proteins, which translocate to the nucleus and participate to the activation of specific target genes. (B) Monomeric Activin binds to type II receptor but does not allow activation. (C) Based on its structure and on overexpression data, model proposing that Atv/Lefty acts as a competitive inhibitor of Activin by interfering with its binding on type II receptor. (D) Increasing the amount of Activin rescues the mesendoderm by competing Atv for the binding and stimulation of the type II activin receptor. (E) Increasing the amount of type II Activin receptor allows the endogenous Activin to bind and stimulate free receptors. (F) Expression of a constitutively activated Type I receptor (TARAM-A^D) stimulates the downstream signaling pathway independently of the presence or absence of Atv.

doses (25-500 pg) of the Activin Receptor type IIa (ARIIA). We then examined the expression of markers of anteroaxial and posteroaxial mesoderm at the end of gastrulation (Fig. 7A,B). Increasing dose of ARIIa RNA resulted in a progressive rescue of both posteroaxial and anteroaxial mesoderm. This rescue strongly suggests that the inhibitory effect of Atv on the Activin signaling pathway does not occur at the level of the ligand but rather results from a competition between Atv and Activin for the stimulation of the Activin receptor.

If this hypothesis is true, the Atv inhibitory effect should be rescued by constitutively stimulating the Activin downstream signaling pathway.

In zebrafish, a constitutively activated serine/threonine kinase receptor related to an Activin type I receptor, TARAM-A^D (Renucci et al., 1996) was shown to induce anteroaxial mesendoderm. Coinjection of Atv (5 pg) with TARAM-A^D (100-500 pg) were performed and the injected embryos were analyzed for the rescue of anteroaxial and posteroaxial mesoderm. In presence of 5 pg antivin RNA and 100 pg TARAM-A^D RNA, 15/123 (44.2%) embryos displayed axial mesoderm whereas at higher dose of TARAM-A^D RNA (500 pg), 212/225 (94.2%) embryos showed axial mesoderm as labelled with *gsc* or *shh* (not shown). When embryos coinjected with Atv and TARAM-A^D were allowed to develop, we observed a rescue of the cyclopia phenotype (Fig. 7E,F), resulting from induction of ventral forebrain by the prechordal mesendoderm and, in the trunk, embryos showed a differentiated notochord (Fig. 7G). When embryos were injected in a saturated manner with Atv (10 pg) at the 2-cell stage followed by a second injection of TARAM-A^D (500 pg) at the 16-cell stage in one lateral blastomere, amongst the embryos showing a rescue of axial mesoderm, 8% (13/162) had a secondary axis. The primary axis was devoid of mesendoderm and displayed a cyclopia phenotype as the result of Atv inhibitory effect, while the secondary axis induced by TARAM-A^D displayed axial mesendoderm and two separate eyes (Fig. 7H).

These experiments demonstrate that a constitutively activated type I receptor is able to rescue Atv inhibition of mesendoderm in a dose-dependent manner. Conversely, for a given amount of TARAM-A^D, increasing antivin RNA up to 200 pg failed to inhibit induction of mesendoderm (not shown). Therefore TARAM-A^D activity is dominant on Atv inhibition of mesendoderm induction.

In conclusion, our study strongly suggests that Atv acts at the level of the binding on Activin receptor and negatively interacts with the Activin signaling pathway.

DISCUSSION

Dynamic expression of *antivin* in structures undergoing inductive processes

Expression of *atv* at blastula stage correlates with expression of *gsc* and *ntl*, which have been shown to be under the control of Activin (Joore et al., 1996; Schulte-Merker et al., 1992). As Atv belongs to a family of signaling molecules, this suggests that it may potentially interact with the Activin signaling pathway (see below).

In its second phase of expression, at gastrulation, *atv*

transcripts are detected in tissues sending out and receiving vertical induction signals, axial mesoderm and ventral neurectoderm namely. At that stage, *atv* expression is very reminiscent of the expression of the *gsc* gene. We have previously hypothesized that *gsc* expression in cephalic neurectoderm may result from a vertical signal coming from mesoderm (Thisse et al., 1994). Therefore, *atv* is a good candidate gene for the induction or regulation of *gsc* expression in the ventral brain.

In its third phase of expression, *atv* transcripts are expressed in a posteroanterior wave along the chordamesoderm suggesting that Atv may be part of a signal, or regulates a signal, emitted by the notochord to induce muscle pioneers in paraxial mesoderm (Halpern et al., 1993) or induces and patterns the ventral neural tube.

The latest phase of *atv* expression is observed in the left heart primordium and the left part of the habenula. In other species, several genes presenting L/R asymmetry have been described. In chick, *activin βB*, *activin receptor type IIA* show right-sided expression, while *shh*, *HNF3β*, and *nodal* are left-sided (Levin, 1997).

In zebrafish, except for *cyclops* which is a zebrafish nodal related factor (Sampath et al., 1998; Rebagliati, 1998), none of these genes are asymmetrically expressed. Whereas L/R asymmetry is already detectable with molecular markers at gastrulation in higher vertebrates, in zebrafish, the first evidence of L/R asymmetry appears around the 18-somite stage, suggesting that, in this species, the breaking of the bilateral symmetry occurs rather late.

Antivin: structure-function relationship

With Lefty and Ebaf, Atv shares the general structure of TGFβs. However, members of this new subgroup of the TGFβ superfamily lack both the large α helix and the seventh cysteine known to be involved in the TGFβ dimerisation, suggesting that these proteins act either as monomers or non-covalent dimers. Lack of the α helix and divergence in the loops of finger tips (known to be involved in the interaction between TGFβs and type II TGFβ receptors, Qian et al., 1994, Griffith et al., 1996) suggest that proteins of the Atv group may either bind a different type of receptor or bind by a different mechanism to TGFβ receptors. Alternatively, proteins of the Atv group may heterodimerize with other TGFβs, preventing them to bind to their own receptors.

Finally, the presence of a large aminoterminal domain may modify the mechanism of action of proteins of the Atv group. Interestingly, the size of the mature peptide is similar to those of in vitro designed dominant-negative forms of other TGFβs such as Activin (Wittbrodt and Rosa, 1994) or BMP4 (Hawley et al., 1995). This suggests that members of the Atv group may function as naturally occurring dominant-negative form of TGFβ.

To understand the implications of these structural characteristics, we analyzed the effect of overexpression of the mouse Lefty in zebrafish embryos. The phenotypes of embryos injected with Lefty or Atv are identical, showing that, despite their poor sequence similarities, the spatial conformations of these two proteins are similar enough to allow Lefty to substitute functionally for Atv in fish. This strongly suggests that Atv and Lefty have the same molecular function in their respective tissues and species and suggest that they have the same physiological target.

Antivin antagonizes the Activin signaling pathway

Induction of mesendoderm involves members of the TGFβs such as Activin or Activin-related factors, which function as covalent dimers and bind to a specific type II receptor. Upon binding, these receptors are activated, interact and phosphorylate a type I receptor, which transduces the signal to downstream elements (Fig. 8A, for review Kretzschmar and Massagué, 1998).

Three hypotheses can be proposed to explain Atv/Lefty interaction with the Activin signaling pathway. First, Atv/Lefty may stimulate its own receptor and, in this case, interaction with Activin will occur at the level of downstream elements. Second, Atv/Lefty may interact with the ligand itself, forming either an inactive heterodimer or either binding to a dimer of Activin, preventing interaction of Activin with the Activin receptor. A similar mechanism has been described for the inhibition of the BMP signaling pathway by Noggin, Chordin and Follistatin (Thomsen, 1997). Third, Atv/Lefty may inhibit the inductive signal by binding competitively to the type II receptor without activating it.

Rescue of the Atv inhibitory effect by ARIIa or by a constitutively activated type I receptor strongly favours the third hypothesis. This mechanism of action is reminiscent of the monomeric activin (Hüsken-Hindi et al., 1994) which, conversely to dimeric Activin, binds to type II receptor but does not activate the downstream signaling pathway (Fig. 8B). Lack of the α helix and the cystein involved in the dimerisation of other TGFβ strongly suggest that Atv/Lefty act as a monomeric form (Fig. 1C) and interact with Activin by competing Activin or Activin-like factors for the binding to their specific receptor (Fig. 8C). This hypothesis is supported by our results as increasing Activin ligand competes efficiently with Atv (Fig. 8D). Similarly, for a given amount of Atv, increasing the amount of type II receptor allows Activin to bind and to stimulate enough free receptor to induce mesendoderm (Fig. 8E). Finally, the stimulation, ligand independent, of the downstream elements of the signaling pathway by a constitutively activated type I receptor is dominant on the inhibition of mesoderm induction by Atv (Fig. 8F).

Antivin-mediated 'knock-out' of mesendoderm reveals the contribution of this germ layer to development of the zebrafish embryo

In the complete absence of mesendoderm resulting from the 'knock out' of the mesodermal induction by overexpression of Atv, embryos develop as an enlarged animal territory which differentiates into epidermis, neural crest and neurectoderm. This expanded ectodermal region is correctly organized along the anteroposterior and dorsoventral axes except that the ventral part of the CNS, which derives from the axial neurectoderm at gastrulation, is missing. This lack of ventral neurectodermal structures directly correlates with loss of axial mesoderm. Effect of axial mesoderm on neurectoderm was also suggested by the phenotypic analysis of two mutations affecting the formation of the anteroaxial mesoderm, *one eye-pinhead* (Schier et al., 1997; Strähle et al., 1997) and *cyclops* (Thisse et al., 1994) for which the lack of ventral CNS structures correlates with a reduction of axial mesoderm. All

these observations strongly suggest that the formation of ventral CNS requires a vertical inductive interaction with the underlying axial mesoderm.

The prechordal plate is the most sensitive mesodermal domain to Atv overexpression. This may reflect that induction of this structure requires the highest dose of Activin (Green et al., 1992; own data). Therefore, decreasing Activin signaling will affect this domain first.

On the contrary, depletion of lateral and ventral mesoderm does not further influence the development of neurectodermal derivatives.

Finally, in the absence of mesendoderm, epiboly and convergence movements occur normally at gastrulation. However, elongation of the embryonic axis is strongly disturbed and anterior cephalic neurectodermal territories rather than differentiating close to the animal pole follow the movement of the margin toward the vegetal region. This demonstrates that mesoderm is required for the correct elongation of the embryonic axis.

To summarize, in addition to its intrinsic function in forming internal organs, the mesoderm appears to be required for the elongation of the embryonic axis and for induction of ventral neurectoderm. On the contrary, other inductive mechanisms occurring at blastula and gastrula stages that define and pattern the ectodermal germ layer along the A/P and D/V axes appear to be independent of mesoderm induction.

We are grateful to Dr J. Wittbrodt and Dr F. Rosa for providing the zebrafish *activinβB* and *TARAM-A^D* cDNAs, to Dr M. Oulad-Abdelghani for the gift of the *lefty* cDNA. We thank Dr S. Wilson for his contribution in the description of Atv expression in the zebrafish brain. We also thank S. Ostertag for her help in analyzing the rescue of axial mesoderm by overexpression of TARAM. Special thanks to Dr M. Halpern, Dr P. Dollé and Dr K. Niederreither for fruitful discussion and comments on the manuscript. We also thank M. Thisse, M. Fürthauer, V. Heyer and T. Steffan for their help along this work and D. Biellmann and O. Nkundwa for maintenance of fish. This work was supported by funds from the Institut National de la Santé et de la Recherche Médicale, the Centre National de la Recherche Scientifique, the Hôpital Universitaire de Strasbourg, the Association pour la Recherche sur le Cancer and the Ligue Nationale Contre le Cancer.

REFERENCES

Barr, P. J. (1991). Mammalian subtilisins: the long-sought dibasic processing endoproteases. *Cell* **66**, 1-3.

Barro, O., Vriz, S., Joly, J.-S., Joly, C., Condamine, H. and Boulekbache, H. (1995). Widespread expression of the evel gene in zebrafish embryos affects the anterior-posterior axis pattern. *Dev. Genetics* **17**, 117-128.

Daopin, S., Piez, K. A., Ogawa, Y. and Davies, D. R. (1992). Crystal structure of transforming growth factor-beta 2: an unusual fold for the superfamily. *Science* **257**, 369-373.

Fürthauer, M., Thisse, C. and Thisse, B. (1997). A role for FGF-8 in the dorso-ventral patterning of the zebrafish embryo. *Development* **124**, 4253-4264.

Green, J. B. A., New, H. J. and Smith, J. C. (1992). Responses of embryonic *Xenopus* cells to activin and FGF are separated by multiple dose thresholds and correspond to distinct axes of the mesoderm. *Cell* **71**, 731-739.

Griffith, D. L., Keck, P., Sampath, T. K., Rueger, D. C. and Carlson, W. D. (1996). Three-dimensional structure of recombinant human osteogenic protein1: structural paradigm for the transforming growth factor b superfamily. *Proc. Natl. Acad. Sci. USA* **93**, 878-883.

Gurdon, J. B., Harger, P., Mitchell, A. and Lemaire, P. (1994). Activin signalling and response to a morphogen gradient. *Nature* **371**, 487-492.

Hammerschmidt, M. and Nüsslein-Volhard, C. (1993). The expression of a zebrafish gene homologous to *Drosophila snail* suggests a conserved function in invertebrate and vertebrate gastrulation. *Development* **119**, 1107-1118.

Halpern, M. E., Ho, R. K., Walker, C. and Kimmel, C. B. (1993). Induction of muscle pioneers and floor plate is distinguishes by the zebrafish *no tail* mutation. *Cell* **75**, 99-111.

Hawley, S. H. B., Wunnenberg-Stapleton, K., Hashimoto, C., Laurent, M. N., Watabe, T., Blumberg, B. W. and Cho, K. W. Y. (1995). Disruption of BMP signals in embryonic *Xenopus* ectoderm leads to direct neural induction. *Genes Dev.* **9**, 2923-2935.

Hüsken-Hindi, P., Tsuchida, K., Park, M., Corrigan, A. Z., Vaughan, J., M., Vale, W. W. and Fischer, W. H. (1994). Monomeric Activin A retains high receptor binding affinity but exhibits low biological activity. *J. Biol. Chem.* **269**, 19380-19384.

Inoue, A., Takahashi, M., Hatta, K., Hotta, Y. and Okamoto, H. (1994). Developmental regulation of *islet-1* mRNA expression during neuronal differentiation in embryonic zebrafish. *Dev. Dyn.* **199**, 1-11.

Joore J., Fasciana C., Speksnijder J. E., Kruijer W., Destree O. H., Van den Eijnden-van Raaij A.J., de Laat S. W. and Zivkovic D. (1996). Regulation of the zebrafish *goosecoid* promoter by mesoderm inducing factors and Xwnt1. *Mech. Dev.* **55**, 3-18.

Kimelman, D. and Kirschner, M. (1987). Synergistic induction of mesoderm by FGF and TGFβ and the identification of an mRNA coding for FGF in the early *Xenopus* embryo. *Cell* **51**, 869-877.

Kimelman, D., Christian, J. L. and Moon, R. T. (1992). Synergistic principles of development: Overlapping patterning systems in *Xenopus* mesoderm induction. *Development* **116**, 1-9.

Kothapalli, R., Buyuksal, I., Wu, S. Q., Chegini, N. and Tabibzadeh, S. (1997). Detection of ebaf, a novel human gene of the transforming growth factor beta superfamily association of gene expression with endometrial bleeding. *J. Clin. Invest.* **99**, 2342-2350.

Kretzschmar, M. and Massagué, J. (1998). SMADs: mediators and regulators of TGF-β signaling. *Curr. Opin. Gen. Dev.* **8**, 103-111.

Levin, M. (1997). Left-right asymmetry in vertebrate embryogenesis. *BioEssays* **19**, 287-296.

Meno, C., Saijoh, Y. Fujii, H., Ikeda, M., Yokoyamas, T., Yokoyama, M., Toyada, Y. and Hamada, H. (1996). Left-right asymmetric expression of the TGFβ-family member *lefty* in mouse embryos. *Nature* **381**, 151-155.

Oulad-Abdelghani, M., Chazaud, C., Bouillet, P., Matteri, M.-G., Dollé, P. and Chambon, P. (1998). Stra3/Lefty, a retinoid acid-inducible novel member of the transforming growth factor-β family. *Int. J. Dev. Biol.* **42**, 23-32.

Qian, S. W., Burmester, J. K., Sun, P. D., Huang, A., Ohlsen, D. J., Suardet, L., Flanders, K. C., Davies, D., Roberts, A. B. and Sporn, M. B. (1994). Characterization of mutated transforming growth factor-βs which possess unique bological properties. *Biochem.* **33**, 12298-12304.

Rebagliati, M.R, Toyama, R., Fricke, C., Haffter, P. and Dawid, I.B. (1998). Zebrafish Nodal-related genes are implicated in axial patterning and establishing left-right asymmetry. *Dev. Biol.* **199**, 261-272.

Renucci, A., Lemarchandel, V. and Rosa, F. (1996). An activated form of type1 serine/threonin kinase receptor TARAM-A reveals a specific signalling pathway involved in fish head organiser formation. *Development* **122**, 3735-3743.

Sampath. K., Rubinstein, A. L., Cheng, A. M., Liang, J. O., Fekany, K., Solnica-Krezel, L., Korzh, V., Halpern, M. E. and Wright, C.V. (1998) Induction of the zebrafish ventral brain and floorplate requires cyclops/nodal signalling. *Nature* **395**, 185-189.

Schier, A. F., Neuhauss, S. C. F., Helde, K. A., Talbot, W. S. and Driever, W. (1997). the *one-eyed pinhead* gene functions in mesoderm and endoderm formation in zebrafish and interacts with no tail. *Development* **124**, 327-342.

Schlunegger, M. P. and Grutter, M. G. (1992). An unusual feature revealed by the crystal structure at 2.2Å resolution of human transforming growth factor-beta 2. *Nature* **358**, 430-434.

Schulte-Merker, S., Ho, R. K., Herrmann, B. G. and Nusslein-Volhard, C. (1992). The protein product of the zebrafish homologue of the mouse *T* gene is expressed in nuclei of the germ ring and the notochord of the early embryo. *Development* **116**, 1021-1032.

Schulte-Merker, S, Hammerschmidt, M., Beuchle, D., Cho, K. W., DeRobertis, E. M. and Nüsslein-Volhard, C. (1994). Expression of zebrafish *goosecoid* and *no tail* gene products in wild-type and mutant no tail embryos. *Development* **120**, 843-852.

Stachel, S., E., Grunwald, D. J. and Myers, P. Z. (1993). Lithium

perturbation and *goosecoid* expression identify a dorsal specification pathway in the pregastrula zebrafish. *Development* **117**, 1261-1274.

Strähle, U., Blader, P, Henrique, D. and Ingham, P. W. (1993). Axial, a zebrafish gene expressed along the developing body axis, shows altered expression in *cyclops* mutant embryos. *Genes Dev.* **7**, 1436-1446.

Strähle, U., Jesuthasan, S., Blader, P., Garcia-Villaba, P., Hatta, K. and Ingham, P. W. (1997). *One-eyed pinhead* is required for development of the ventral midline of the zebrafish (*Danio rerio*) neural tube. *Genes Function* **1**, 131-148.

Thisse, C., Thisse, B., Schilling, T. F. and Postlethwait, J. H. (1993). Structure of the zebrafish *snail1* gene and its expression in wild-type, *spadetail*, and *no tail* mutant embryos. *Development* **119**, 1203-1215.

Thisse, C., Thisse, B., Halpern, M. E. and Postlethwait, J. H. (1994). *goooseсoid* expression in neurectoderm and mesendoderm is disrupted in zebrafish *cyclops* gastrulas. *Dev. Biol.* **164**, 420-429.

Thomsen, G. Woolf, T., Whitman, M., Sokol, S., Vaughan, J., Vale, W. and Melton, D. A. (1990). Activins are expressed early in *Xenopus* embryogenesis and can induce axial mesoderm and anterior structures. *Cell* **63**, 485-493.

Thomsen, G.H. (1997). Antagonism within and around the organizer: BMP inhibitors in vertebrate body patterning. *Trends Genet.* **13**, 209-211.

Wittbrodt, J. and Rosa, F. (1994). Disruption of mesoderm and axis formation in fish by ectopic expression of activin variants: the role of maternal activin. *Genes Dev.* **8**, 1448-1462.